



저작자표시-비영리-변경금지 2.0 대한민국

이용자는 아래의 조건을 따르는 경우에 한하여 자유롭게

- 이 저작물을 복제, 배포, 전송, 전시, 공연 및 방송할 수 있습니다.

다음과 같은 조건을 따라야 합니다:



저작자표시. 귀하는 원저작자를 표시하여야 합니다.



비영리. 귀하는 이 저작물을 영리 목적으로 이용할 수 없습니다.



변경금지. 귀하는 이 저작물을 개작, 변형 또는 가공할 수 없습니다.

- 귀하는, 이 저작물의 재이용이나 배포의 경우, 이 저작물에 적용된 이용허락조건을 명확하게 나타내어야 합니다.
- 저작권자로부터 별도의 허가를 받으면 이러한 조건들은 적용되지 않습니다.

저작권법에 따른 이용자의 권리는 위의 내용에 의하여 영향을 받지 않습니다.

이것은 [이용허락규약\(Legal Code\)](#)을 이해하기 쉽게 요약한 것입니다.

[Disclaimer](#)

**Development of a biomarker-based
prediction model of disease progression
during chemotherapy in children and
adolescents**

Young-A Heo

Department of Medical Science

The Graduate School, Yonsei University

**Development of a biomarker-based
prediction model of disease progression
during chemotherapy in children and
adolescents**

Young-A Heo

Department of Medical Science

The Graduate School, Yonsei University

**Development of a biomarker-based
prediction model of disease progression
during chemotherapy in children and
adolescents**

Directed by Professor Kyungsoo Park

The Doctoral Dissertation

submitted to the Department of Medical Science,

the Graduate School of Yonsei University

in partial fulfillment of the requirements for the degree of

Doctor of Philosophy

Young-A Heo

December 2016

This certifies that the Doctoral
Dissertation of Young-A Heo is approved

Thesis supervisor: Kyungsoo Park

Thesis committee Member #1: Chuhl Joo Lyu

Thesis committee Member #2: Sang Joon Shin

Thesis committee Member #3: Nick Holford

Thesis committee Member #4: Ja Seung Koo

The Graduate School

Yonsei University

December 2016

ACKNOWLEDGEMENTS

Firstly, I would like to give my deepest gratitude to my supervisor, Professor Kyungsoo Park for his constructive guidance, endless support and excellent encouragement throughout my PhD years. The completion of this thesis would have not been possible without Professor Park's help.

I would also like to show my greatest gratitude to Professor Chuhl Joo Lyu, Professor Sang Joon Shin and Professor Ja Seung Koo for their help and examining the thesis. I would also like to thank Professor Nick Holford for supporting me and guide me during my times as a visiting academics in New Zealand. I thoroughly enjoyed the time and learnt valuable lessons from him.

I would like to give many thanks to the Professors in the Pharmacology lab in giving advice through seminars and staff members to look after the students with care. I really enjoyed my time with them throughout the project.

I would also like to thank all the PhD students in our lab: Mijeong, Dong Woo, Jinju and Yoonsub who helped and supported me during the project.

Finally, I would like to thank my family, relatives and friends for all the support they gave me with endless love and the Lord who carried me throughout my PhD years.

2016 Young-A Heo

TABLE OF CONTENTS

ABSTRACT	2
I. INTRODUCTION.....	5
1. Pharmacokinetic-pharmacodynamic (PKPD) modeling in oncology	5
2. Role of biomarkers in oncology	6
3. Acute lymphoblastic Leukemia (ALL)	7
4. Prognostic factors of ALL	8
5. Study purposes	9
II. MATERIALS AND METHODS	10
1. Patients and data collections	10
2. Model development	11
<i>A. Categorization</i>	<i>11</i>
<i>B. Baseline model for biomarkers</i>	<i>12</i>
(1) Indirect response model.....	15
(2) Proliferation cell model	15
<i>C. Drug effect model</i>	<i>17</i>
<i>D. Disease dynamics</i>	<i>18</i>
<i>E. Chemotherapy resistance.....</i>	<i>22</i>
<i>F. Covariate analysis</i>	<i>24</i>
<i>G. Overall survival analysis.....</i>	<i>24</i>
<i>H. Estimation method.....</i>	<i>25</i>
3. Model selection and evaluation.....	25
III. RESULTS	26
1. Patient demographics and data.....	26

2. PKPD modeling of ALC	2 7
3. PKPD modeling of PLT	3 1
4. Overall survival analysis	3 5
IV. DISCUSSION	3 7
V. CONCLUSION	4 1
REFERENCES	4 2
ABSTRACT (IN KOREAN)	4 6

LIST OF FIGURES

Figure 1. Observations of mean value of ALC (*1000/mm ³) over time (days) in ALL.	1 4
Figure 2. Observations of mean value of PLT (*1000/mm ³) over time (days) in ALL.	1 4
Figure 3. The structural pharmacodynamics model describing the chemotherapy-induced changes of biomarker proliferations adopted from Friberg et al.	1 7
Figure 4. The structural pharmacodynamics model describing the chemotherapy-induced changes of biomarker proliferations with disease level adopted from Buil-bruna et al and Friberg et al.	1 9
Figure 5. The structural pharmacodynamics model describing the chemotherapy-induced changes of biomarker synthesis with disease level adopted from Desmee et al.	2 0
Figure 6. The structural pharmacodynamics model describing the chemotherapy-induced changes of biomarker proliferations with disease level adopted from Hansson et al and Friberg et al.	2 1
Figure 7. A goodness of fit plot for the final model of ALC where CWRES represents conditional weighted residual and population predictions represents the model prediction.	3 0
Figure 8. VPC plots of disease progression model of ALC (right) and the same model without a disease progression term (left). Observations and predictions are illustrated in red lines and black lines respectively. Solid lines represent median, lower and upper dashed lines represent 5th	

percentile and 95th percentile respectively. Shaded areas describe 95% confidence interval of the predictions. 3 0

Figure 9. A goodness of fit plot for the final model of disease progression of PLT where CWRES represents conditional weighted residual and population predictions represents the model prediction. 3 4

Figure 10. VPC plots of disease progression model of PLT (right) and the same model without a disease progression term (left). Observations and predictions are illustrated in red lines and black lines respectively. Solid lines represent median, lower and upper dashed lines represent 5th percentile and 95th percentile respectively. Shaded areas describe 95% confidence interval of the predictions. 3 4

Figure 11. Kaplan-Meier plot of overall survival data. Observations are illustrated in black lines and shaded areas describe 95% prediction intervals of the Kaplan-Meier plot. Base hazard was described by a constant model ($\lambda=0.0173$) and applied in the simulations. 3 6

LIST OF TABLES

Table 1. Known important prognostic factors in ALL in children ¹¹	9
Table 2. Risk stratification for ALL in children and adolescents.....	1 2
Table 3. Demographic characteristics of study subjects for population PK analysis	2 6
Table 4. Estimated parameters of disease progression of ALC (*1000/mm ³) before maintenance therapy.....	2 8
Table 5. Estimated parameters of disease progression of PLT (*1000/mm ³) before maintenance therapy.....	3 2
Table 6. Model parameter estimates for 3 year overall survival of ALL patients	3 6

LIST OF ABBREVIATIONS

ALC	Absolute Lymphocyte Count
ALL	Acute lymphoblastic leukemia
ALT(SGOT)	Alanine Transaminase
AST(SGPT)	Aspartate Transaminase
BMT	Bone marrow transplantation
D_{PLT}	Predicted disease slope of PLT at day 30
D_{ALC}	Predicted disease slope of ALC at day 30
IRB	Institutional Review Board, 연구심의위원회
LYM	Lymphocyte
NONMEM	Non-linear mixed effects modeling
OS	Overall survival
PKPD	Pharmacokinetic-pharmacodynamic
PLT	Platelet Count
PsN	Perl speaks NONMEM
R_{ALC}	Predicted mean ALC ratio to baseline over day 1 to day 22
RBC	Red Blood Cell
SCM	Step wise covariate model building
WBC	White Blood Cell
WBCC	White Blood Cell Count
WFN	Wings for NONMEM
VPC	Visual Predictive Check

ABSTRACT

Development of a biomarker-based prediction model of disease progression during chemotherapy in children and adolescents

Young-A Heo

*Department of Medical Science
The Graduate School, Yonsei University*

(Directed by Professor Kyungsoo Park)

Aims: This study aims to develop a quantitative semi-mechanistic model to describe the disease progression of leukemia during chemotherapy using circulating biomarkers in Korean children and adolescent population.

Methods: A routine clinical data set for 74 patients who were diagnosed as acute lymphoblastic leukemia (ALL) for the first time between the age of 1 – 19 were collected from Severance hospital electric medical records (EMR) system. Absolute lymphocyte count (ALC) and platelet count (PLT) were dependent variables. Age, WBC count, bone marrow transplantation (BMT) and other laboratory results such as creatinine, AST and ALT levels were possible covariates to be tested. A (semi) mechanistic model was used to describe ALC and PLT changes with time during chemotherapy. A K-PD model was used to describe drug kinetics as blood concentration data were not available. ALC and PLT production were described by a

single compartment representing proliferative cells, 3 transit compartments representing biomarker maturation, and a single compartment representing biomarker concentrations in blood, where ALC production was assumed to be positively influenced by linear disease progression of ALL and reduced by chemotherapy and vice versa for PLT. Covariate search was then carried out for biomarkers. Population modeling approach was performed using NONMEM 7.3. 3 year overall survival analysis was performed using variables from biomarker disease progression models as predictors of overall survival of ALL patients.

Results: Due to data's heterogeneity, patients treatment options were grouped into risk based protocol, standard risk (SR) and high risk (HR) based on the clinical practice. Drug effect was described by an E_{max} model of effect-site concentration obtained from K-PD model, where drug doses were BSA standardized due to the use of multiple cytotoxic drugs during the treatment. In addition, chemotherapy resistance was described the best with inhibitory I_{max} model where the chemotherapy exposure inhibits the drug effect. Estimated EC_{50} of standard and high risk groups are 0.00026 and 0.711 respectively in ALC, and 1.57 and 3.1 respectively in PLT. Estimated mean transit time (MTT) was 5.34 days and 17.0 days for lymphocyte and platelet respectively. Estimated gamma for ALC and PLT were 0.0973 and 0.215 respectively, which denotes the power of feedback component. For 3 year survival analysis of ALL patients, predicted latent disease slope of PLT at day 30 (D_{PLT}), history of bone marrow transplantation (BMT) and predicted ALC/baseline ratio averaged over the period of day 1 to day 22 (R_{ALC}) were statistically significant predictors of 3 yr survival time in ALL patients in children and adolescents.

Conclusion: The proposed semi-mechanistic disease progression model with circulating biomarkers provide platforms to predict survival time of ALL patients

which can be a powerful tool to help clinicians to monitor disease in ALL patients in children and adolescents.

Keywords: acute lymphoblastic leukemia, biomarker, disease progression model, platelet counts, absolute lymphocyte counts, clinical data

I. INTRODUCTION

1. Pharmacokinetic-pharmacodynamic (PKPD) modeling in oncology

In recent years, development of individualized therapies for oncology patients became the key objective to enhance efficacy.¹ By doing so, it is hoped that the individualized therapy would be able to predict a clinical outcome from an early stage when the patients were given existing or newly developed treatment.¹ Unfortunately, the difficulty lies in the various factors influencing outcome such as treatment efficacy, toxicity and development of resistance and the limited predictive ability of current monitoring techniques.²

For cancer patients, extending overall survival (OS) is considered to be the most preferred endpoint to examine treatment benefit but collecting OS data may take years before drawing statistical conclusion. As a result, drug development is often based on an improvement in progression free survival (PFS).² Population PKPD modeling has become a key tool in drug development including oncologic drugs to understand, identify and quantify various dose-response relationships.² The modeling techniques provide platform to predict the time course of the drug effect with the aim to optimize dosing^{2,3} and links the drug effect to tumor growth dynamics. By doing so, it can be used to discriminate drug effects from degenerative disease.^{2,4} In addition, PKPD modeling can describe between subject variability and quantitatively account for covariate influence thus drug effect on the disease can be evaluated more precisely.

After all, developed PKPD models in clinical oncology may aid clinicians to individualize drug treatment scheme and industry to design clinical trials towards minimizing drug toxicity and optimize drug efficacy through establishing optimal dose, regimen for individual patient.

2. Role of biomarkers in oncology

Recently, applying circulating biomarkers that are known to be related to the pathophysiology of cancer to quantitatively predict the clinical outcome is proposed as an alternative approach.¹⁻³ Circulating biomarkers are fairly easy to obtain from peripheral blood and can be used in conjunction with conventional diagnostic method and procedure such as RECIST.¹ Despite the fact that proof of concept regarding the use of biomarkers is well-established in drug development,^{2,3} use of biomarkers to evaluate the treatment response is seldom applied in clinical practice possibly due to inadequate validation of biomarkers.

Therefore, in order to properly assess the utility of biomarkers, assessments should be made in the context of longitudinal models linking their observed levels with clinical outcome in a timely manner. Recently, few studies showed the feasibility of the use of longitudinal models with (semi) mechanistic approaches.^{1,5-10} There have been approaches to develop population modeling of tumor size or tumor markers to assess the efficacy of oncologic drugs on cancer.^{1,4,7-10}

Hansson et al successfully developed the population disease progression model to predict the change in tumor size by using longitudinal biomarker as one of predictors of tumor dynamics in gastrointestinal stromal tumors (GIST), receiving sunitinib and/or placebo treatment.⁹ Buil-Bruna et al developed a population

pharmacodynamics model to predict the tumor progression in Small Cell Lung Cancer (SCLC) patients using lactate dehydrogenase (LDH) and neuron specific enolase (NSE).¹ The developed model comprised of two parts, disease level and biomarkers turnover models and one of the key assumptions for the model is that the progression of the diseases promotes the synthesis of LDH and NSE. On the other hand, Desmee et al demonstrated that complex and physiological models can be used to improve treatment evaluation and prediction in oncology. The literature suggested the idea by developing joint model that determines the relationship between time to event and PSA kinetics mechanistically.¹⁰

3. Acute lymphoblastic Leukemia (ALL)

ALL is a malignant disease of the bone marrow where early lymphoid precursors proliferate and replace the normal hematopoietic cells of the marrow.¹¹ It is the most common cancer among children and adolescents.¹¹ Patients with ALL commonly present with symptoms including bleeding due to thrombocytopenia and fatigue from anemia.¹¹ The disease could be of B-cell precursor or T-cell lineage and patients with T-cell lineage shows inferior survival among children and adolescents.

Childhood ALL generally comprises multiple genetic alterations including aneuploidy or DNA sequence mutations. These mutations commonly target genes encoding proteins that are involved in tumor-suppressor functions, lymphoid differentiation and cell signaling. Major progress has been made in the management of ALL, especially with the introduction of multi agent chemotherapy by which, survival rate increased from 10% in the 1960s to almost 90% in 2000s.^{11,12}

4. Prognostic factors of ALL

Prognostic factors could be an indicator for considering the intensity of chemotherapy at diagnosis and the selection of patients in first remission for bone marrow transplantation. Major prognostic factors in ALL include the biologic and genetic features of leukemia cells, clinical features that are present at diagnosis and the early response to chemotherapy (Table 1).¹¹

In addition, circulating biomarkers have recently been emerging as important prognostic factors to predict the overall survival.¹³⁻¹⁶ Elevated serum LDH level at diagnosis has been consistently identified as an independent prognostic factor linked with poor survival.^{14,15,17}

Wulantingsih et al found inverse association between LDH and patient survival where higher pre-diagnostic LDH levels corresponded to lower cancer-specific survival following cancer diagnosis.¹⁷ Furthermore, there have been studies to indicate that the time to platelet recovery is an essential component of complete remission in acute lymphoblastic leukemia.^{16,18} Faderl et al showed the possibility of platelet recovery time as an independent prognostic factor to determine the disease free and overall survival.¹⁶ Also, lymphocyte recovery has been recently known to be a possible independent prognostic factor for overall survival of ALL.^{19,20} However, PKPD models of biomarkers to link and predict the disease progression of ALL and treatment efficacy have not been studied over.

Table 1. Known important prognostic factors in ALL in children ¹¹

Variable	Favorable	Unfavorable
Clinical features		
Age (years)	1 < age < 10	1 > age ≥ 10
Sex	Female	Male
Initial white-cell count	< 50,000 /mm ³	≥ 50,000 /mm ³
Biologic or genetic features of leukemia cells		
Immunophenotype	B-cell	T-cell
Cytogenetic features	ETV6-RUNX1, hyperdiploidy	BCR-ABL1, hypodiploidy
Early response to treatment		
Response to 1 week of glucocorticoid therapy	Good response	Poor response
Bone marrow morphology after 1 to 2 weeks of multi agent chemotherapy	M1 marrow (< 5% blasts) by day 8 or 15	No M1 marrow (≥ 5 % blasts) by day 8 or 15

5. Study purposes

The objective of the study is to develop a disease progression model, utilizing circulating biomarkers in pediatric patients with ALL. It is hypothesized that with (semi) mechanistic approaches, the developed disease progression models will increase the reliability of biomarkers in predicting disease dynamics.

II. MATERIALS AND METHODS

1. Patients and data collections

The study was conducted with retrospectively collected data from Severance Hospital, Seoul, Korea. Total of 74 patients' data whom were diagnosed with ALL at the age of less than 20 were obtained from Electrical Medical Records. Patients with comorbidities were excluded in the study. It was a 52 week study, consisting of multiple cycles of chemotherapy before maintenance therapy and bone marrow transplantation during the treatment if necessary. Patients were dropped out from the study if they had relapses or deceased during the follow up. The study was approved by the Institutional Review Board of Severance Hospital.

Three different biomarker candidates were first selected as possible endpoints for the analysis. Platelet count (PLT), LDH level and absolute lymphocyte count (ALC) were chosen according to literature search.^{12,13,15,16} However observations suggested that LDH lacked specificity in ALL thus it was excluded from the analysis (data not shown).

Platelet count (PLT) and absolute lymphocyte count (ALC) at plasma level were the endpoints to be analyzed in this work. PLT were collected from a full red blood cell (RBC) count and ALC were collected from a full white blood cell (WBC) count. ALC were calculated from WBC counts and differential blood cell count percentages. RBC and WBC were assessed in the clinical laboratory of the Severance Hospital. Measurements were collected at the time of ALL diagnosis and up to 52 weeks after the diagnosis.

Blood samples for drug concentration were not available but the dosage information for each cycle was collected. Other laboratory results and hematological counts such as serum creatinine, uric acid and neutrophil count were collected. Disease status, demographic data such as age, gender and body weight were also collected as possible covariates.

2. Model development

ALC and PLT measured in plasma were analyzed by nonlinear mixed effects modeling. The model consisted of structure model and random effects model. The structure model would describe the typical patient level kinetics and dynamics of biomarkers. The random effects model would estimate inter patient variation and random unexplained variability such as measurement error. Four different structure models were proposed to describe the disease progression and treatment efficacy in patients with ALL in children and adolescents.

A. Categorization

To treat ALL, chemotherapy with multiple anticancer agents was proved to be more effective than monotherapy.^{21,22} Patients were stratified into two risk groups (standard and high risk). Criteria to stratify patients into risk groups were listed in Table 2. Depending on their initial risk, patients can receive slightly different combination of anticancer agents with different duration at each cycle. Treatments generally consisted of standard drugs such as prednisone, methotrexate, cytarabine, cyclophosphamide, vincristine and L-asparaginase. Unless the treatment toxicity was lethal, all patients received standard doses that were stratified by body surface area (BSA). Chemotherapy regimen consisted of 4 phases, induction, consolidation,

intensification and maintenance therapy. In addition to multi agent chemotherapy, some patients received cranial irradiation and/or bone marrow transplantation if appropriate.^{11,18} Study population were stratified according to risk groups for the analysis.

Table 2. Risk stratification for ALL in children and adolescents

Standard Risk	- WBC counts are less than 50,000/ μ l or
	- Diagnosed at the age between 2 to 9 or
	- In the absence of CNS metastasis, mediastinal mass or
	- No t(9:22), biphenotypic leukemia and dupMLL arrangements
High Risk	- WBC counts are higher than 50,000/ μ l or
	- Diagnosed at the age less than 1 or over 10 or
	- Presence of CNS metastasis, mediastinal mass or
	- T-cell phenotype, t(9:22), biphenotypic leukemia and dupMLL arrangements or
	- Not achieved complete remission after remission induction therapy

B. Baseline model for biomarkers

Figure 1 and Figure 2 described the typical absolute lymphocyte count (ALC) and platelet count (PLT) profile obtained from the ALL patients. Observed ALC at the diagnosis were above the reference range and decreased following the treatment. Decrease in ALC reflected the treatment related improvement in ALL, leading to a decrease in the synthesis rate of the ALC. Slight fluctuations and increase of ALC at the end of study period (after 250 days) despite the ongoing chemotherapy may

indicate the resistance effects. Unlike ALC, PLT was below the reference range at the diagnosis of ALL and the concentrations increases following the treatment. Increase in PLT reflected the treatment related improvement in ALL, leading to an increase in the synthesis rate of PLT. The fundamental assumptions in the model for each biomarker were as the followings:

- The progression of the disease lead to increase in lymphocyte counts
- Chemotherapy inhibit lymphocyte stimulation
- The progression of the disease lead to decrease in platelet counts
- Chemotherapy elicit platelet recovery

The assumption was based on the observations as shown in Figure 1 and Figure 2. ALC and PLT profiles were described in two different form of turnover models, indirect response model ²³ and proliferation model adopted from Friberg et al.²⁴

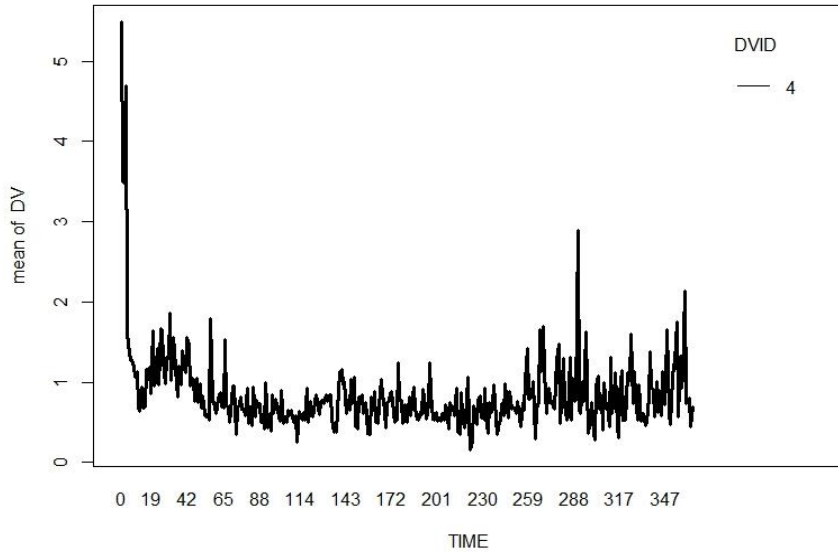


Figure 1. Observations of mean value of ALC ($*1000/\text{mm}^3$) over time (days) in ALL.

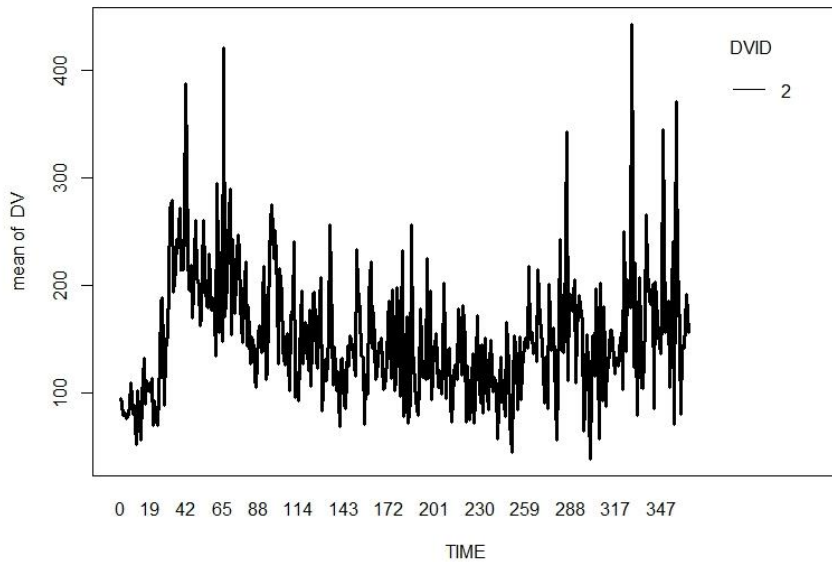


Figure 2. Observations of mean value of PLT ($*1000/\text{mm}^3$) over time (days) in ALL.

(1) Indirect response model

ALC and PLT dynamics were described with indirect response models²³ in the forms of Equation 1 and Equation 2.

$$\frac{dALC}{dt} = K_{in} \times (1 - E_{drug}) - K_{out} \times ALC(t) \quad \text{Equation 1}$$

$$\frac{dPLT}{dt} = K_{in} \times (1 + E_{drug}) - K_{out} \times PLT(t) \quad \text{Equation 2}$$

Where K_{in} is a zero order synthesis rate constant of biomarkers and K_{out} is a first order degradation rate constant of biomarkers. E_{drug} , represents the drug effects and the main assumptions were that the drug effect decreases the synthesis rate of ALC (Equation 1) and increases the synthesis rate of PLT (Equation 2).

(2) Proliferation cell model

ALC and PLT dynamics were described with proliferation model to mimic the life span of both biomarkers from bone marrow production in Equation 3 - Equation 9 below (Equation 3 applies to ALC, Equation 4 to PLT and the rest to both biomarkers). The structure model was adopted from Friberg et al.²⁴ The schematic diagram of proliferation cell model was illustrated in Figure 3. The structure model comprised of five compartments where one compartment represented progenitor cells of biomarkers (Prol), three transit compartments with maturing biomarkers (Transit) and a compartment of circulating biomarkers observed in plasma.

$$\frac{dProl}{dt} = K_{prol} \times Prol(t) \times (1 - E_{drug}) \times \left(\frac{Circ0}{Circ}\right)^{\gamma} - K_{tr} \times Prol(t) \quad \text{Equation 3}$$

$$\frac{dProl}{dt} = K_{prol} \times Prol(t) \times (1 + E_{drug}) \times \left(\frac{Circ0}{Circ}\right)^{\gamma} - K_{tr} \times Prol(t) \quad \text{Equation 4}$$

$$\frac{dTransit1}{dt} = K_{tr} \times Prol(t) - K_{tr} \times Transit1 \quad \text{Equation 5}$$

$$\frac{dTransit2}{dt} = K_{tr} \times Transit1 - K_{tr} \times Transit2 \quad \text{Equation 6}$$

$$\frac{dTransit3}{dt} = K_{tr} \times Transit2 - K_{tr} \times Transit3 \quad \text{Equation 7}$$

$$\frac{dCirc}{dt} = K_{tr} \times Transit3 - K_{circ} \times Circ \quad \text{Equation 8}$$

$$MTT = \frac{4}{K_{tr}} \quad \text{Equation 9}$$

K_{prol} is a proliferation rate constant that determines the rate of proliferative cell divisions of progenitor cells of biomarkers. $(\frac{Circ0}{Circ})^\gamma$ mimicked the feedback mechanism from the circulating biomarkers to describe the rebound of biomarkers and $Prol(t)$ is an amount of progenitor cells over time. It is assumed that the only loss of cells in the transit compartments is into the next compartment (Equation 5 - Equation 8). At steady state, $\frac{dProl}{dt} = 0$ thus K_{prol} is equal to rate constant K_{tr} . Friberg et al further assumed that K_{circ} is equal to K_{tr} to minimize the number of parameters. For easier interpretation, the mean transit time (MTT) was estimated as shown in Equation 9 where n is the number of transit compartments. E_{drug} represents the drug effects and the main assumptions were that the drug effect decreases the synthesis rate of ALC (Equation 3) and increases the synthesis rate of PLT (Equation 4).

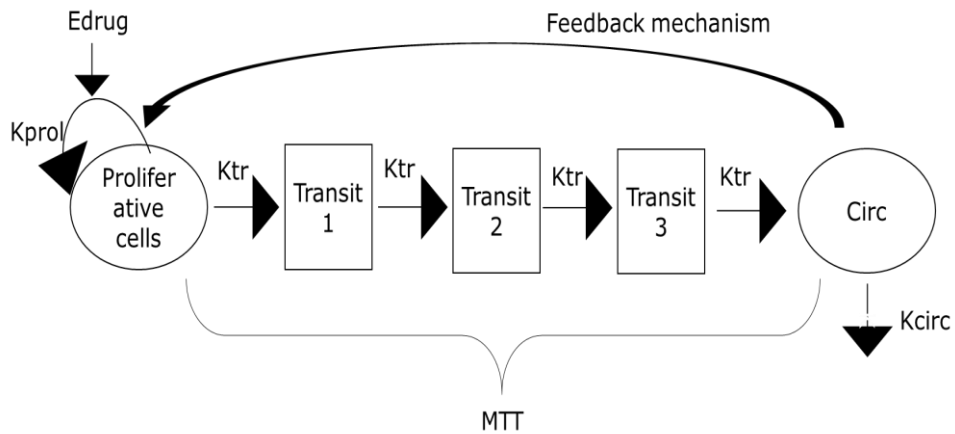


Figure 3. The structural pharmacodynamics model describing the chemotherapy-induced changes of biomarker proliferations adopted from Friberg et al.

C. Drug effect model

Due to a complex regimen to treat ALL, wide range of dose units and the fact that the standard dose of anticancer agents were used in each cycle, dose of each drug was set to 1 to describe the administration of chemotherapy. Each dose was generally standardized on the basis of BSA, the nominal dose of 1 was multiplied by the patient's BSA then divided by the standard BSA (BSA_{std}), 1.73 m^2 (Equation 10). Each dose was assumed to be administered with a dosing interval of 1 day.

Drug concentrations were not available therefore K-PD approach was applied with theoretical allometry approach (Equation 11 and Equation 12). $A(t)$ is the BSA standardized hypothetical drug amount of chemotherapy and K is the first order elimination rate constant with theoretical allometry approach as shown in Equation 12. WT and WT_{std} is the weight of individual patient and standard weight of 70 kg respectively. Treatments were assumed to enhance or reduce the turnover rate of

biomarkers by the function E_{drug} , which was modeled to be either a linear function (Equation 14) or an E_{max} model (Equation 15). CE represents the hypothetical drug exposure to chemotherapy divided by nominal volume (WT/W_{tstd}) (Equation 13). E_{max} is the maximum inhibition effect and EC_{50} is the nominalized concentration which produced 50% maximum inhibition.

$$DOSE = 1 \times \frac{BSA}{BSA_{std}} \quad \text{Equation 10}$$

$$\frac{dA}{dt} = -K \times A(t) \quad \text{Equation 11}$$

$$K = K_{std} \times \left(\frac{WT}{WT_{std}}\right)^{0.25} \quad \text{Equation 12}$$

$$CE = \frac{A(t)}{V} \quad \text{Equation 13}$$

$$E_{drug} = Slope \times CE \quad \text{Equation 14}$$

$$E_{drug} = E_{max} \times \frac{CE}{CE + EC_{50}} \quad \text{Equation 15}$$

D. Disease dynamics

Three different disease latent approaches were used to describe the latent disease dynamics of ALL (D), with transit and circulating compartments as described in Equation 5 - Equation 9 being incorporated. First disease dynamic model was adopted from Buil-bruna et al ¹ whose schematic diagram is shown in Figure 4 and model equations in Equation 16 - Equation 18.

$$\frac{dD}{dt} = \alpha \times D(t) - E_{drug} \quad \text{Equation 16}$$

$$\frac{dALC}{dt} = ((K_{prol} \times ALC(t))/(1 + K_D \times D(t))) \times \left(\frac{Circ0}{Circ}\right)^y - K_{tr} \times ALC(t) \quad \text{Equation 17}$$

$$\frac{dPLT}{dt} = ((K_{prol} \times PLT(t)) \times (1 + K_D \times D(t)) \times \left(\frac{Circ0}{Circ}\right)^y - K_{tr} \times PLT(t) \quad \text{Equation 18}$$

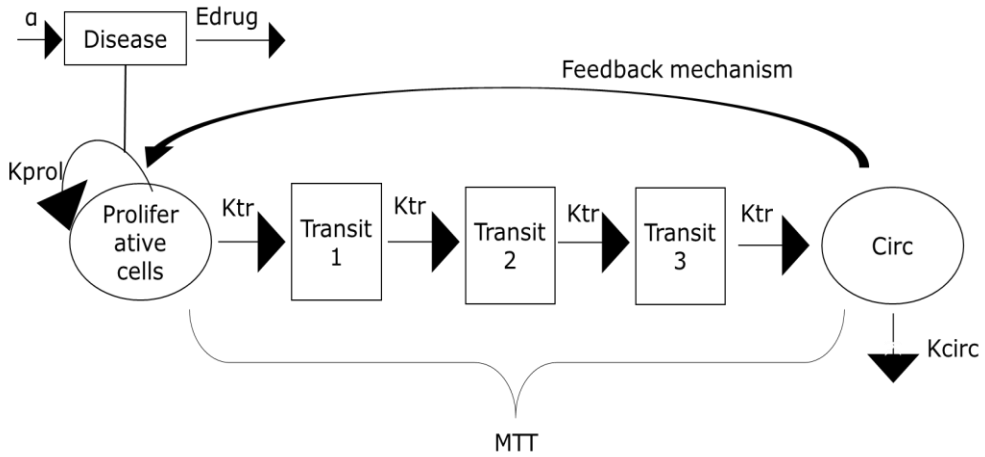


Figure 4. The structural pharmacodynamics model describing the chemotherapy-induced changes of biomarker proliferations with disease level adopted from Builbruna et al and Friberg et al.

Equation 16 defines the unperturbed dynamics of disease level of ALL. It describes that a natural history of ALL progress exponentially with the net growth rate of alpha (α). The disease level at diagnosis was set to 1 in all patients. Drug model (Edrug) was assumed to cause irreversible reduction on the net growth rate of ALL (Edrug = $\alpha \times CE \times D(t)$). Disease dynamics were then incorporated into proliferation cell model described in Equation 17 - Equation 18. Scaling constant (K_D) and disease levels over time ($D(t)$) were added in the proliferative cell compartment. It was

assumed that the disease level, $D(t)$ increased the synthesis rate of the proliferative cells of ALC and decreased the synthesis rate of the proliferative cells of PLT.

Second approach was adopted from Desmee et al ¹⁰ whose schematic diagram is shown in Figure 5 and model equations in Equation 19 - Equation 21.

$$\frac{dD}{dt} = r \times (1 - Edrug)D(t) - d \times D(t) \quad \text{Equation 19}$$

$$\frac{dALC}{dt} = Kin + p \times D(t) - Kout \times ALC(t) \quad \text{Equation 20}$$

$$\frac{dPLT}{dt} = Kin + \left(\frac{p}{(1 + D(t))} \right) - Kout \times PLT(t) \quad \text{Equation 21}$$

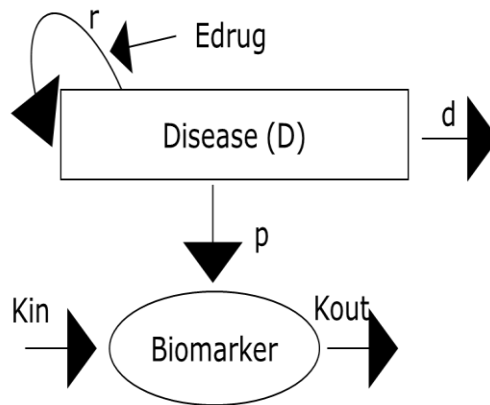


Figure 5. The structural pharmacodynamics model describing the chemotherapy-induced changes of biomarker synthesis with disease level adopted from Desmee et al.

The model consisted of a separate compartment for disease level and the biomarker concentrations are described as turnover model. In the absence of treatment, the model assumed that the disease level (D) grows with the rate r and are eliminated with rate d (Equation 18). It is assumed that the chemotherapy for ALL (Edrug) acts by decreasing growth rate r . In the literature, Edrug was restricted to be between 0 and 1. Increased disease level escalates biomarker level with a production rate (p), which is synthesized with endogenous zero order synthesis rate (K_{in}) and cleared from the plasma with first order elimination rate (K_{out}). It is assumed that the disease level, $D(t)$ increases the production of ALC and decreases the production of PLT (Equation 20 and Equation 21).

Lastly, Hansson et al was developed whose schematic diagram is shown in Figure 6 and model equations in Equation 22 - Equation 25.

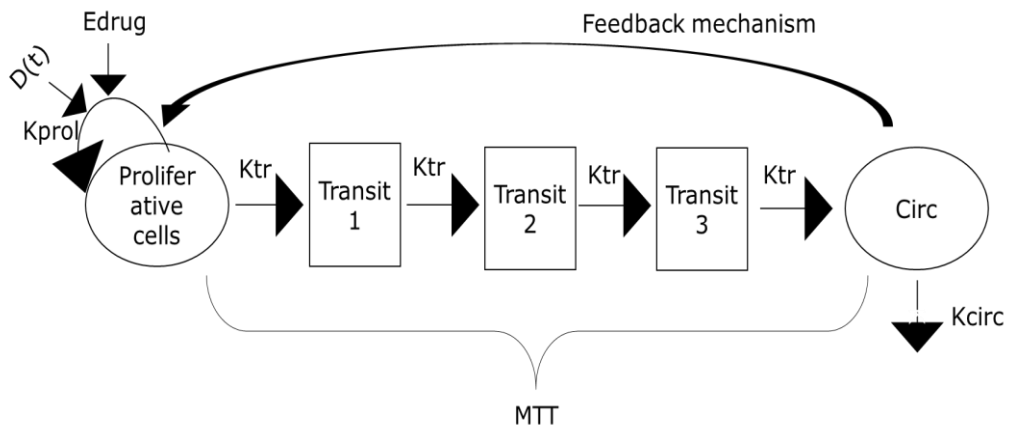


Figure 6. The structural pharmacodynamics model describing the chemotherapy-induced changes of biomarker proliferations with disease level adopted from Hansson et al and Friberg et al.

$$D(t) = ALC \times (1 + D_{slope} \times t) \quad \text{Equation 22}$$

$$D(t) = \frac{PLT}{(1 + D_{slope} \times t)} \quad \text{Equation 23}$$

$$\frac{dALC}{dt} = K_{prol} \times D(t) \times (1 - Edrug) \times \left(\frac{Circ0}{Circ}\right)^{\gamma} - K_{tr} \times ALC(t) \quad \text{Equation 24}$$

$$\frac{dPLT}{dt} = K_{prol} \times D(t) \times (1 + Edrug) \times \left(\frac{Circ0}{Circ}\right)^{\gamma} - K_{tr} \times PLT(t) \quad \text{Equation 25}$$

In this approach, disease progression model is used to determine the role of biomarkers as predictors of tumor dynamics.⁹ Hansson et al proposed that the disease progressions ($D(t)$) within untreated patients were described by a linear disease progression model dependent on time (t) with a slope parameter (D_{slope}) affecting the biomarker concentrations. It is assumed that the disease progression increases the synthesis rate of proliferative cells of ALC (Equation 24) and decreases the synthesis rate of proliferative cells of PLT (Equation 25). The disease dynamics are then incorporated into proliferation cell model described in Equation 24-25. Disease level is multiplied to K_{prol} to alter the synthesis rate of proliferative cells of biomarkers.

E. Chemotherapy resistance

Treatment resistance term was included in the chosen basic disease progression model to account for the resurgence in circulating biomarker levels observed in the dataset. It was assumed that the treatment resistance was in relation to the cumulative chemotherapy exposure or the area under concentration curve (AUC) for the hypothetical effect-site concentration (CE) (Equation 13). Equation 26 describes the

AUC for CE from zero to each evaluation time point. Three different approaches were taken to describe the drug treatment resistance.

First the exposure was assumed to decrease exponentially with the scale parameter γ as shown in Equation 27. The other approach assumed that tolerance develops in proportion to CE and disappears in the first order resistance development constant (KR) as shown in Equation 28. Then the tolerance effect was applied as inhibiting the drug effect as shown in Equation 29. In addition, extra I_{\max} drug model (Equation 30) representing the tolerance effect was subtracted from the drug effect as shown in Equation 31. Resistance effect was only described with the selected basic disease progression model that best described the data.

$$AUC = \int CE(t) \quad \text{Equation 26}$$

$$R = e^{-\gamma \times AUC} \quad \text{Equation 27}$$

$$\frac{dTOL}{dt} = KR \times CE - KR \times TOL \quad \text{Equation 28}$$

$$Edrug = \frac{Emax \times \frac{CE}{CE + EC50}}{(1 + TOL)} \quad \text{Equation 29}$$

$$Rdrug = RImax \times \frac{TOL}{TOL + RIC50} \quad \text{Equation 30}$$

$$Edrug = Emax \times \frac{CE}{CE + EC50} - Rdrug \quad \text{Equation 31}$$

F. Covariate analysis

Parameter-covariate relationships were graphically and statistically tested preliminarily with the basic disease progression model. The selection procedure was conducted separately for each biomarker. A stepwise covariate model building approach (SCM) was performed afterward using PsN at significance levels of $p < 0.05$ for forward selection and $p < 0.01$ for backward elimination.²⁵ The criteria of the statistical test were based on the χ^2 -distribution.²⁶

Potential covariates were searched based on previous studies where its relevance to biomarker levels or ALL were clinically known or had been studied and proven to be important. Those included demographic factors such as age and gender and laboratory results such as serum creatinine, aspartate aminotransferase (AST), alanine aminotransferase (ALT) and uric acid.^{11,27-30} AST and ALT were included in the covariate analysis, largely to evaluate the impact of liver and hepatic dysfunction on chemotherapy efficacy.

G. Overall survival analysis

Different distributions (constant, log-logistic, weibull and gompertz) were evaluated to describe the baseline hazard. Predicted latent disease progression slopes at day 30 from PLT disease progression models (i.e., D_{slope} in Equation 22) and mean ALC ratio to baseline predicted from ALC disease progression model were introduced as covariates.

$$h(t) = h_0(t) \times e^{\delta \times B_i} \quad \text{Equation 32}$$

Where $h_0(t)$ it the baseline hazard, δ is the parameter to be estimated and B_i is a set of possible predictors of survival time in each individual, i . Possible predictors are

the estimated parameters from circulating biomarker disease progression models and the history of bone marrow transplantation and age at diagnosis.

H. Estimation method

All PKPD analyses were done with NONMEM (Version 7.3, ICON, Hanover, MD) and the first order conditional estimation with the interaction option. Survival model was analyzed with the first order method. Visual predictive checks (VPCs) were created using Wings for NONMEM 740. PsN version 3.4.2 and Xpose implemented in R was used for SCM and graphical representation

3. Model selection and evaluation

Model selection was guided by the precision of parameter estimates, objective function value (OFV) and Akaike Information criterion (AIC). To verify that the final population PKPD models adequately described the central tendency and spread of the data, the models were evaluated using a goodness of fit plots and VPC plots given 1,000 simulated datasets from the final models. Observed biomarker concentrations were overlaid with model predictions (mean, 5th and 95th percentiles) to detect the fraction of the data that lay within the model prediction intervals.³¹ Kaplan-Meier VPC plots were plotted to evaluate the survival analysis model.³²

III. RESULTS

1. Patient demographics and data

Data were available from 74 children and adolescents who were diagnosed with ALL for disease progression model. A summary of the demographic characteristics of study population is reported in Table 3. For K-PD approach, there were 7429 data points of drug administration. A mean of 100 dosing points were taken from each patient (range 31 to 201). There were 2810 measurements of ALC and 2840 measurements of PLT. On average, each patient contributed 38 points on average for both ALC and PLT (range 19 to 56 and 20 to 57 for ALC and PLT respectively).

Table 3. Demographic characteristics of study subjects for population PK analysis

Biomarkers	Dataset (n=74)
ALC ¹ (*1000/mm ³)	157±54.1
PLT ¹ (*1000/mm ³)	1.02±0.39
Continuous	
Age at diagnosis ¹ (years)	6.3±3.79
Weight ¹ (kg)	24.8±13.6
AST ¹ (IU/L)	42.3±24.3
ALT ¹ (IU/L)	58.76±35.6
Creatinine ¹ (mg/dL)	0.44±0.13
Uric acid ¹	2.27±3.06
Categorical	
Gender (Y/N)	37/37

Risk group (Standard/High)	26/48
Bone marrow transplantation (Y/N)	38/36

¹ Values are expressed as mean \pm SD

2. PKPD modeling of ALC

Represented model in Figure 6 best described the dynamics of ALC in plasma over time. Different approaches for disease dynamics provided poorer fit to the data in terms of graphical analysis and AIC. The core assumption of this model is that the disease linearly progress with time, the disease dynamics will increase the synthesis of ALC and drug treatment will reduce the effect of disease progression. Addition of chemotherapy resistance further improved the fit graphically where extra I_{\max} drug model was added to account for the reduced efficacy (Equation 30) and chosen as a final basic model to describe the disease progression with ALC. SCM was carried out and age was chosen as significant covariates to explain the variability of mean transit time of lymphocyte maturation from bone marrow to plasma. In addition, white blood cell count (WBCC) was selected to describe the uncertainty in ALC at baseline progenitor cells where the baseline decreases with age over 5.11 years. No covariates were deleted from backward deletion and no other relationships that were tested in SCM showed statistical significant effects.

The AIC value of the selected model was -244.056 where the graphical fit was the best out of all the tested models. The OFV of final disease progression model was -286.056 and the significance of P-value from basic model was < 0.0001 (Δ OFV: 34.785). Data supported the estimation of between subject variability for baseline, E_{\max} , EC_{50} , mean transit time (MTT), disease slope and drug half-life estimated from the PKPD model. Between subject variability ranged from 31.3% to 242.7%,

reflecting the high heterogeneity of the data. Proportional error model best described the residual unidentified variability in the data.

The estimated disease progression model parameters for ALC are listed in Table 4. Estimated EC_{50} is 0.00026 for standard risk group and 0.711 for high risk group. Estimated slope to describe the linear progression of the ALL that affects the synthesis rate of proliferation cells of ALC is 0.00003 per day. Estimated KR is 0.0203 per day indicating the rather slow onset of chemotherapy resistance of about 49.3 days. A goodness of fit plot of the selected final model is drawn in Figure 7 and shows that the model is in a relatively good agreement with the data.

The disease progression model of ALC was evaluated by VPC. The confidence interval of the ALC predictions was consistent with the median observations (Figure 8). To further evaluate the appropriateness of the model, the selected disease progression model was compared to the model without disease progression slope as shown in Figure 8. A VPC using a model with the slope of disease progression fixed to 0 were almost same at predicting the upper quartile but was worse at predicting the median. Overall, the model with disease slope parameter was better at describing the time course of ALC especially at the median and lower quartiles.

Table 4. Estimated parameters of disease progression of ALC (*1000/mm³) before maintenance therapy

OFV (AIC)	-286.056 (-244.056)
No. of Parameter	21
Parameter	Structural parameters (RSE(%))

Baseline ($10^3/\text{mm}^3$)	1.81 (10.6)
Covariate: WBCC	0.173 (5.8)
E_{max}*	0.125 (11.6)
SR_EC₅₀*	0.00026 (146.9)
HR_EC₅₀*	0.711 (36.7)
MTT (day)	5.34 (5.1)-
Covariate: Age	0.0818 (27.8)
γ	0.0973 (11.3)
Disease slope (/day)	0.00003 (37.3)
T half life (day)	18.8 (22.4)
KR (/day)	0.0203 (58.1)
T_Imax*	0.0191 (33.5)
TIC₅₀*	0.112 (188.4)
Parameter	Between subject variability (RSE(%))
ω Baseline (CV(%))	52.5 (13.6)
ω E_{max}(CV(%))	31.3 (19.2)
ω EC₅₀(CV(%))	140.7 (20.6)
ω MTT(CV(%))	242.7 (16.2)
ω Disease slope (CV(%))	109.1 (23.8)
ω T half life (CV(%))	122.9 (18.4)
Parameter	Residual variability (RSE(%))
σ Proportional (CV(%))	62.3 (1.6)

*: unitless variables as real dosing information was not used and hypothetical amount was applied instead.

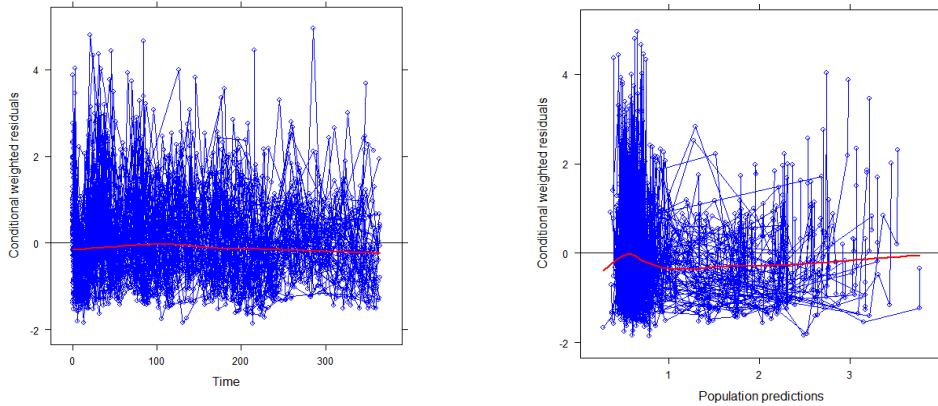


Figure 7. A goodness of fit plot for the final model of ALC where CWRES represents conditional weighted residual and population predictions represents the model predictions.

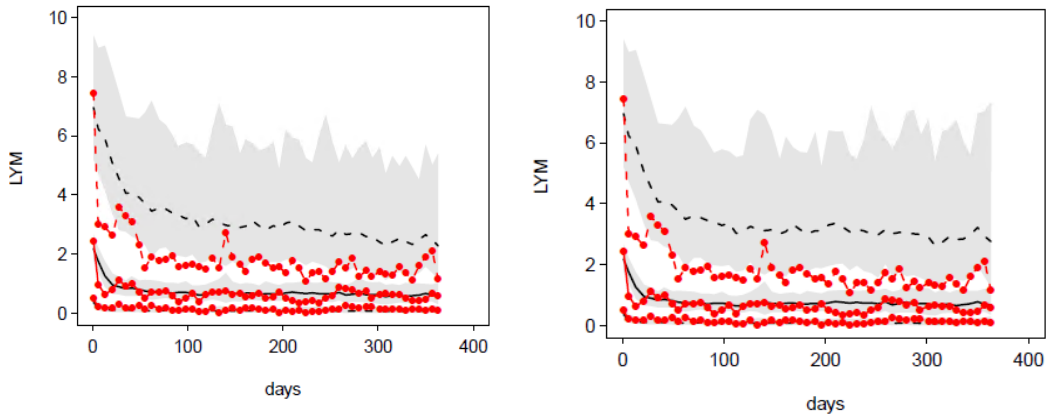


Figure 8. VPC plots of disease progression model of ALC (right) and the same model without a disease progression term (left). Observations and predictions are illustrated in red lines and black lines respectively. Solid lines represent median, lower and upper dashed lines represent 5th percentile and 95th percentile respectively. Shaded areas describe 95% confidence interval of the predictions.

3. PKPD modeling of PLT

Represented model in Figure 6 best described the dynamics of PLT in plasma over time and was selected as a final basic model. The core assumption of this model is that the disease progress linearly with time and the disease dynamics will decrease the synthesis of PLT and drug treatment will reduce the effect of disease progression. Addition of chemotherapy resistance further improved the model fit when extra I_{\max} drug model was added to account for the reduced chemotherapy efficacy due to resistance (Equation 30) and chosen as a final basic model to describe the disease progression with PLT. SCM was carried out and ALT, AST and creatinine was chosen as significant covariates to explain the variability of drug half-life for K-PD model. In addition, age was selected to describe the uncertainty in platelet counts at baseline where the baseline increases if the patient is over 5.24 years. No covariates were deleted from backward deletion and no other relationships that were tested in SCM showed statistical significant effects.

The AIC value of 28295.284 for the selected model was the lowest which demonstrated that the chosen model best described the data. The OFV of final disease progression model was 28249.284 and the significance of P-value from basic model was < 0.0001 (Δ OFV: 150.098). Between subject variability for baseline, E_{\max} , EC_{50} , mean transit time (MTT), disease slope and drug half-life were estimated. Between subject variability ranged from 27.9% to 160.3%, reflecting the high dispersion of the data. Proportional error model best described the residual unidentified variability in the data.

The estimated disease progression model parameters for PLT are listed in Table 5. Estimated EC_{50} of standard risk group is 1.02 and 3.1 for high risk group. Slope to describe the linear progression of the disease that affects the synthesis rate of

proliferation cells of PLT is 0.0000671 per day. Estimated KR is 0.0912 per day indicating the rather fast onset of chemotherapy resistance of about 11.0 days. A goodness of fit plot of the selected final model is drawn and the plots is in a relatively good agreement with the data (Figure 9).

The disease progression model of PLT was evaluated by VPC. The confidence interval of the PLT concentration predictions was consistent with the median observations (Figure 10). The model seemed to capture the overall shape and the dispersion of the data well except upper quartiles. To further evaluate the appropriateness of the model, the selected disease progression model was compared to the model without disease progression slope (Figure 10). A VPC using a model with the slope of disease progression fixed to 0 was not so markedly different but nevertheless, the model with disease slope parameter was better at describing the time course of PLT especially at the upper quartiles with narrower confidence intervals.

Table 5. Estimated parameters of disease progression of PLT (*1000/mm³) before maintenance therapy

OFV (AIC)	28249.284(28295.284)
No. of Parameter	23
Parameter	Structural parameters (RSE(%))
Baseline (10³/mm³)	62.8 (15.5)
Covariate:Age	0.173 (93.1)
E_{max}*	1.02 (14.3)
SR_EC₅₀*	1.57 (39.4)
HR_EC₅₀*	3.1 (33.2)
MTT (day)	17 (2.3)

γ	0.215 (5.0)
Disease slope (/day)	0.0000671 (52.2)
T half life (day)	29.9 (3.2)
Covariate: AST1	0.0192 (10.3)
Covariate: AST2	0.0347 (21.3)
Covariate:ALT	-0.335 (16.4)
Covariate: Creatinine	0.135 (131.1)
KR (/day)	0.0912 (23.1)
TImax*	0.738 (19.4)
TIC ₅₀ *	3.13 (17.9)

Parameter	Between subject variability (RSE(%))
ω Baseline (CV(%))	67.3 (13.5)
ω Emax(CV(%))	13.9 (24.5)
ω EC ₅₀ (CV(%))	100.5 (24.4)
ω MTT(CV(%))	27.9 (14.2)
ω disease slope (CV(%))	160.3 (20.2)
ω T half life (CV(%))	122.9 (17.5)
Parameter	Residual variability (RSE(%))
σ Proportional (CV(%))	57.8 (2.0)

*: unitless variables as real dosing information was not used and hypothetical amount was applied instead.

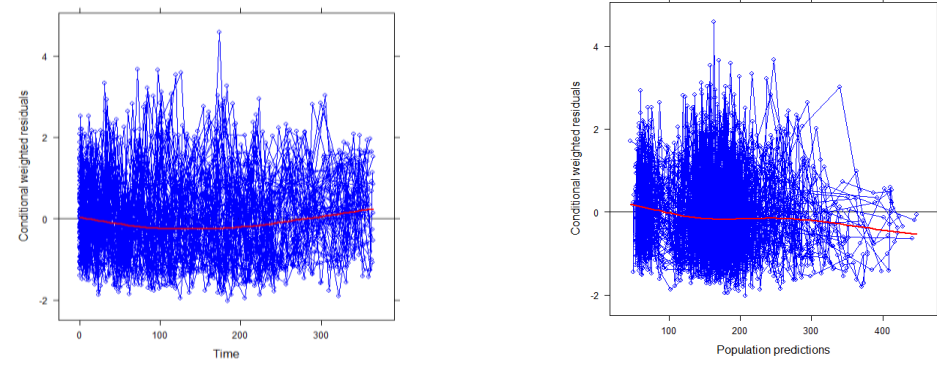


Figure 9. A goodness of fit plot for the final model of disease progression of PLT where CWRES represents conditional weighted residual and population predictions represents the model prediction

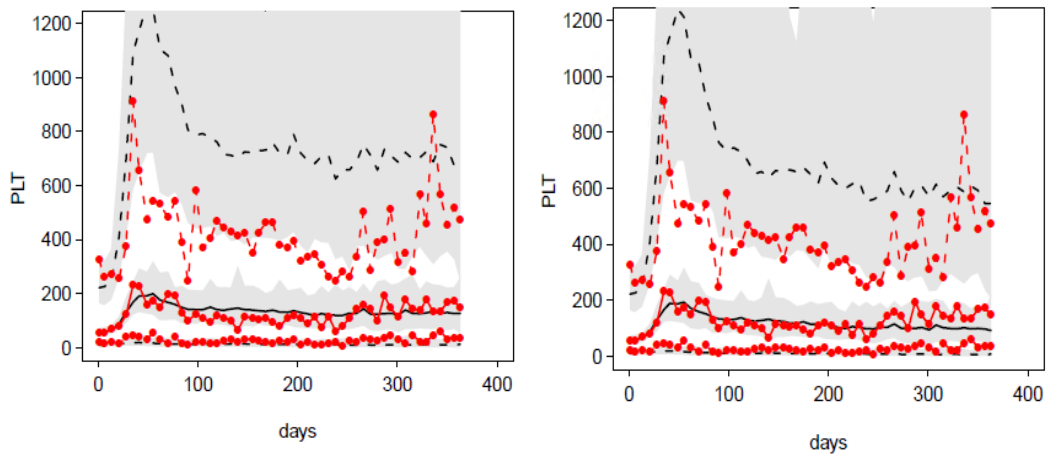


Figure 10. VPC plots of disease progression model of PLT (right) and the same model without a disease progression term (left). Observations and predictions are illustrated in red lines and black lines respectively. Solid lines represent median, lower and upper dashed lines represent 5th percentile and 95th percentile respectively. Shaded areas describe 95% confidence interval of the predictions.

4. Overall survival analysis

A constant hazard model best described the underlying baseline hazard distributions of 3 year overall survival of ALL patients. Predicted latent disease slope of PLT at day 30 (D_{PLT}) and predicted ALC ratio to baseline averaged over the period of day 1 to day 22 (R_{ALC}) were statistically significant predictors of overall survival. Inclusion of history of bone marrow transplantation (BMT) further improved the model fit, in terms of OFV (Equation 34). Inclusion of these covariates decreased the likelihood by 23.372 points.

$$h_0(t) = \lambda \quad \text{Equation 33}$$

$$h(t) = h_0(t) \times e^{\delta 1 \times D_{PLT} + \delta 2 \times R_{ALC} + \delta 3 \times BMT} \quad \text{Equation 34}$$

Predicted latent disease slope of ALC at day 30 (D_{ALC}) was a significant predictor of overall survival when tested individually but was no longer significant when other predictors were included in the model. Estimated parameters for overall survival analysis are reported in Table 6. Increases in latent disease slope of PLT and ALC ratio smaller than 0.8 were associated with an increased mortality. Performance of BMT further increased the risk of death.

The VPC of the survival model with a Kaplan-Meier plot with the simulated 95% confidence interval shows good predictive performance (Figure 11).

Table 6. Model parameter estimates for 3 year overall survival of ALL patients

OFV	127.885
No. Parameter	4
Structural Parameters (RSE(%))	
λ (/month)	0.0173 (105.2)
δ_1	25.7 (14.9)
δ_2	1.87 (32.5)
δ_3	-2.91 (47.4)
Variance Parameters	
ω (CV%)	0 FIX

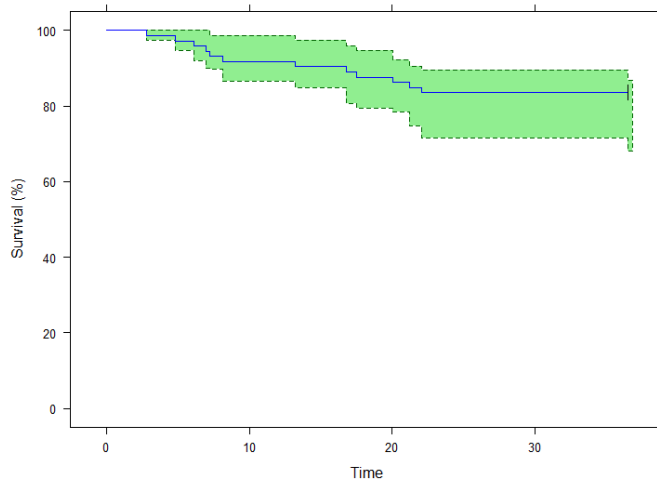


Figure 11. Kaplan-Meier plot of overall survival data. Observations are illustrated in blue lines and shaded areas describe 95% prediction intervals of the Kaplan-Meier plot. Base hazard was described by a constant model ($\lambda=0.0173$) and applied in the simulations.

IV. DISCUSSION

Novel serum biomarkers have been emerging as promising predictive value in relations to oncology.^{1,33} Development of mechanistic models are particularly important to characterize the time course of biomarkers since the relations between biomarker concentrations and disease progression are often not be linear and straightforward.¹

ALC and PLT are frequently measured in routine practice and there have been many studies that published the importance of ALC and PLT as important prognostic factors.^{12,13,16,18,20,34,35} Published studies generally used one or two time points to review the role of biomarkers as a significant predictor in ALL. Rabin et al reviewed ALC at several time points during induction therapy and concluded that the patients with ALC higher than 1,500 cells/ μ l at day 29 had a superior 6-year relapse free survival and overall survival.²⁰ Zeidler et al on the other hand focused the relevance of normal blood counts during early treatment phase of ALL. The study found that the platelet count on treatment day 33 after induction therapy significantly associated with treatment outcome.¹⁸ Our study focused on the time course of ALC and PLT instead of few time points as there are no studies that analyzed the predictive value of longitudinal data of ALC and PLT in relations to clinical outcomes of ALL.

Selected disease progression models are capable of describing the longitudinal data of ALC and PLT in a biological manner where the maturation of biomarker from the bone marrow to the plasma is described by semi-mechanistic model adopted from Friberg et al.²⁴ In addition, disease progression of ALL is described to directly affect the synthesis of proliferative cells in the bone marrow as ALL is a malignant disease

of the bone marrow where early lymphoid precursors proliferate and replace the normal hematopoietic cells of the marrow.

In this study, it is assumed that the disease progression increases the synthesis of lymphocyte proliferative cells and decreases the synthesis of platelet proliferative cells as the early clinical symptoms include thrombocytopenia and raised WBC counts¹¹. These assumptions are rather crude to describe the complex biological processes of maturation of selected biomarkers but it is believed that they will be sufficient to capture the major process influencing longitudinal data of biomarkers. Estimated slope of disease progression on proliferation rate of biomarkers is 0.00003 per day and 0.0000671 per day for ALC and PLT respectively. The estimated values are rather small but the findings are important that the evolving disease clearly affects the proliferation rate of biomarkers in bone marrow.

In the model, a reduction or progression of ALL is reflected in a change of biomarker concentrations. Chemotherapy is considered to directly influence production of lymphocyte and platelet in the bone marrow which indirectly effects the concentrations at plasma. Estimated EC_{50} of chemotherapy for ALC and PLT are higher in the high risk group than the standard risk group. Risk groups are stratified according to the known prognostic factors of ALL (Table 2) and that a patient is classified to a severe risk group (ie. High risk) if the known prognostic factors such as WBC and age are unfavorable.¹¹ As a result, estimated parameter results from the models are in accordance with findings from a previously published studies regarding ALL¹¹ where higher estimated value of EC_{50} indicate more complex regimen of chemotherapy are required or that the ALL is more persistent and takes longer for the treatment to be effective.

Development of chemotherapy resistance is described in the terms of inhibitory I_{\max} model that reduces the overall efficacy of E_{\max} drug model over time. Half-life to develop chemotherapy resistance is estimated to be about 49.3 days in ALC and estimated I_{\max} is 0.0129 which is about 10 times lower than the estimated E_{\max} of drug model. These findings can be an indication that the drug resistance may only hinder up to 10% of maximum treatment effect which could be due to multiple use of cytotoxic drugs.^{11,21,35} However in terms of PLT, half-life to develop chemotherapy resistance is estimated to be about 11.0 days and estimated I_{\max} is 0.738 which can inhibit up to 70% of estimated E_{\max} of drug model. These findings can be an indication that the drug resistance may be exhibited more quickly through PLT than ALC.

AST, ALT and creatinine were shown to affect the half-life of chemotherapy treatment in PLT which is consistent with literature where impaired liver or renal function may change the metabolism and/or elimination of drugs from the body.^{28,34,36} Age is a significant covariate to explain variability in baseline of biomarker PLT and mean transit time of ALC. It is expected as age is a proven prognostic factor of ALL and influence the baseline value or maturation time of biomarkers which can possibly be an indirect marker of ALL progression.^{11,18,20}

The data was generally representative of ALL patients in children and adolescents as the survival rate of current dataset (83%) was similar to the reported survival rate in the literature.¹¹ Attempts to predict overall survival based on changes in biomarker concentrations showed that the model-predicted parameters or biomarker responses in PLT and ALC based on longitudinal data can be used as an additive tool to monitor disease in ALL patients in children and adolescents. The findings can be supported by the published literature where the time to platelet recovery from thrombocytopenia and ALC ratio at day 29 were shown to be important predictors of overall survival.^{16,20}

For the developed model, since longitudinal data of ALC were applied, mean ALC ratio over day 1 to day 22 was sufficient to be a powerful predictor of 3 year survival of ALL patients in children and adolescents.

Developed models in this project have several limitations. First of all, the treatment options from gathered patients were very heterogeneous and patients in high risk group were presented with genetic variations. Further work should be carried out to subset high risk group according to genetic variations. Treatment effect was established through K-PD model due to lack of pharmacokinetic data and this may mask the possible interactions between anticancer agents and individual exposure variability of drugs. In addition, the predictive performance of the disease progression model may vary in the clinical settings where individual patient's characteristics vary greatly but addition of covariates in the model could be sufficient to explain the variability. External validation should be carried out in further studies to evaluate the performance capability of the developed models. Another limitation is that due to the nature of data recollection from clinical setting, maintenance therapy period could have been included in some of the patients from few days up to few weeks. However, intensity of the biomarker measurements were sparse towards the maintenance therapy and must not have impacted the results to build the biomarker disease progression models.

Despite its limitations, the study developed a modeling framework that allowed integration of the time course of circulating biomarker responses during disease progression. In addition, predicted biomarker responses were shown to be important predictors of survival time in ALL patients in children and adolescents. The framework approach does not only enables predictions of survival time for further use within other pediatric ALL patients but can also be applied to other indications.

V. CONCLUSION

E_{\max} model with K-PD theoretical allometry approach, inhibitory I_{\max} model of development of chemotherapy resistance, proliferation model of biomarkers and linear disease progression on synthesis rate of proliferative cells adequately describe the longitudinal data of ALC and PLT in children and adolescents with ALL. Predicted latent disease slope of PLT, predicted mean ALC ratio to baseline and history of BMT were found to be the most promising variables as predictors of survival time of ALL patients. It is believed that the modeling circulating biomarkers could be a useful tool to monitor disease of ALL in children and adolescents.

REFERENCES

- 1 Buil-Bruna, N., Lopez-Picazo, J. M., Moreno-Jimenez, M., Martin-Algarra, S., Ribba, B. & Troconiz, I. F. A population pharmacodynamic model for lactate dehydrogenase and neuron specific enolase to predict tumor progression in small cell lung cancer patients. *The AAPS journal* **16**, 609-619, doi:10.1208/s12248-014-9600-0 (2014).
- 2 Bender, B. C., Schindler, E. & Friberg, L. E. Population pharmacokinetic-pharmacodynamic modelling in oncology: a tool for predicting clinical response. *British journal of clinical pharmacology* **79**, 56-71, doi:10.1111/bcp.12258 (2015).
- 3 Danhof, M., Alvan, G., Dahl, S. G., Kuhlmann, J. & Paintaud, G. Mechanism-based pharmacokinetic-pharmacodynamic modeling—a new classification of biomarkers. *Pharmaceutical research* **22**, 1432-1437, doi:10.1007/s11095-005-5882-3 (2005).
- 4 Simeoni, M., Magni, P., Cammia, C., De Nicolao, G., Croci, V., Pesenti, E. *et al.* Predictive pharmacokinetic-pharmacodynamic modeling of tumor growth kinetics in xenograft models after administration of anticancer agents. *Cancer research* **64**, 1094-1101 (2004).
- 5 Faloppi, L., Scartozzi, M., Bianconi, M., Svegliati Baroni, G., Toniutto, P., Giampieri, R. *et al.* The role of LDH serum levels in predicting global outcome in HCC patients treated with sorafenib: implications for clinical management. *BMC cancer* **14**, 110, doi:10.1186/1471-2407-14-110 (2014).
- 6 Kogan, Y., Halevi-Tobias, K., Elishmereni, M., Vuk-Pavlovic, S. & Agur, Z. Reconsidering the paradigm of cancer immunotherapy by computationally aided real-time personalization. *Cancer research* **72**, 2218-2227, doi:10.1158/0008-5472.CAN-11-4166 (2012).
- 7 Romero, E., Velez de Mendizabal, N., Cendros, J. M., Peraire, C., Bascompta, E., Obach, R. *et al.* Pharmacokinetic/pharmacodynamic model of the testosterone effects of triptorelin administered in sustained release formulations in patients with prostate cancer. *The Journal of pharmacology and experimental therapeutics* **342**, 788-798, doi:10.1124/jpet.112.195560 (2012).
- 8 You, B., Fronton, L., Boyle, H., Droz, J. P., Girard, P., Tranchand, B. *et al.* Predictive value of modeled AUC(AFP-hCG), a dynamic kinetic parameter characterizing serum tumor marker decline in patients with nonseminomatous germ cell tumor. *Urology* **76**, 423-429 e422, doi:10.1016/j.urology.2010.02.049 (2010).

- 9 Hansson, E., Amantea, M., Westwood, P., Milligan, P., Houk, B., French, J. *et al.* PKPD Modeling of VEGF, sVEGFR-2, sVEGFR-3, and sKIT as predictors of tumor dynamics and overall survival following sunitinib treatment in GIST. *CPT: pharmacometrics & systems pharmacology* **2**, 1-9 (2013).
- 10 Desmée, S., Mentré, F., Veyrat-Follet, C. & Guedj, J. Nonlinear mixed-effect models for prostate-specific antigen kinetics and link with survival in the context of metastatic prostate cancer: a comparison by simulation of two-stage and joint approaches. *The AAPS journal* **17**, 691-699 (2015).
- 11 Hunger, S. P. & Mullighan, C. G. Acute Lymphoblastic Leukemia in Children. *The New England journal of medicine* **373**, 1541-1552, doi:10.1056/NEJMra1400972 (2015).
- 12 Donadieu, J., Auclerc, M. F., Baruchel, A., Leblanc, T., Landman-Parker, J., Perel, Y. *et al.* Critical study of prognostic factors in childhood acute lymphoblastic leukaemia: differences in outcome are poorly explained by the most significant prognostic variables. Fralle group. French Acute Lymphoblastic Leukaemia study group. *British journal of haematology* **102**, 729-739 (1998).
- 13 Cheng, Y. P., Luo, Z. B., Yang, S. L., Jia, M., Zhao, H. Z., Xu, W. Q. *et al.* The ratio of absolute lymphocyte count at interim of therapy to absolute lymphocyte count at diagnosis predicts survival in childhood B-lineage acute lymphoblastic leukemia. *Leukemia Res* **39**, 144-150, doi:10.1016/j.leukres.2014.11.013 (2015).
- 14 Miao, P., Sheng, S., Sun, X., Liu, J. & Huang, G. Lactate dehydrogenase A in cancer: a promising target for diagnosis and therapy. *IUBMB life* **65**, 904-910, doi:10.1002/iub.1216 (2013).
- 15 Suh, S. Y. & Ahn, H. Y. Lactate dehydrogenase as a prognostic factor for survival time of terminally ill cancer patients: a preliminary study. *European journal of cancer* **43**, 1051-1059, doi:10.1016/j.ejca.2007.01.031 (2007).
- 16 Faderl, S., Thall, P. F., Kantarjian, H. M. & Estrov, Z. Time to platelet recovery predicts outcome of patients with de novo acute lymphoblastic leukaemia who have achieved a complete remission. *British journal of haematology* **117**, 869-874 (2002).
- 17 Wulaningsih, W., Holmberg, L., Garmo, H., Malmstrom, H., Lambe, M., Hammar, N. *et al.* Serum lactate dehydrogenase and survival following cancer diagnosis. *British journal of cancer* (2015).
- 18 Zeidler, L., Zimmermann, M., Mörlicke, A., Meissner, B., Bartels, D., Tschann, C. *et al.* Low platelet counts after induction therapy for childhood acute lymphoblastic leukemia are strongly associated with poor early response to treatment as measured by minimal residual disease and are prognostic for treatment outcome. *Haematologica* **97**, 402-409 (2012).

- 19 Defoiche, J., Debacq, C., Asquith, B., Zhang, Y., Burny, A., Bron, D. *et al.* Reduction of B cell turnover in chronic lymphocytic leukaemia. *British journal of haematology* **143**, 240-247 (2008).
- 20 Rabin, K. R., Gramatges, M. M., Borowitz, M. J., Palla, S. L., Shi, X., Margolin, J. F. *et al.* Absolute lymphocyte counts refine minimal residual disease-based risk stratification in childhood acute lymphoblastic leukemia. *Pediatric blood & cancer* **59**, 468-474 (2012).
- 21 LeClerc, J. M., Billett, A. L., Gelber, R. D., Dalton, V., Tarbell, N., Lipton, J. M. *et al.* Treatment of childhood acute lymphoblastic leukemia: results of Dana-Farber ALL Consortium Protocol 87-01. *Journal of clinical oncology : official journal of the American Society of Clinical Oncology* **20**, 237-246 (2002).
- 22 Redaelli, A., Laskin, B., Stephens, J., Botteman, M. & Pashos, C. A systematic literature review of the clinical and epidemiological burden of acute lymphoblastic leukaemia (ALL). *European journal of cancer care* **14**, 53-62 (2005).
- 23 Jusko, W. J., Ko, H. C. & Ebling, W. F. Convergence of direct and indirect pharmacodynamic response models. *Journal of pharmacokinetics and biopharmaceutics* **23**, 5-8; discussion 9-10 (1995).
- 24 Friberg, L. E., Henningson, A., Maas, H., Nguyen, L. & Karlsson, M. O. Model of chemotherapy-induced myelosuppression with parameter consistency across drugs. *Journal of clinical oncology* **20**, 4713-4721 (2002).
- 25 Wahlby, U., Jonsson, E. N. & Karlsson, M. O. Comparison of stepwise covariate model building strategies in population pharmacokinetic-pharmacodynamic analysis. *AAPS pharmSci* **4**, E27, doi:10.1208/ps040427 (2002).
- 26 Beal, S. L., Sheiner, L. B., Boeckmann, A. J. & Bauer, R. J. NONMEM users guides. *NONMEM Project Group, University of California, San Francisco* (1992).
- 27 Shin, H. S., Lee, H. R., Lee, D. C., Shim, J. Y., Cho, K. H. & Suh, S. Y. Uric acid as a prognostic factor for survival time: a prospective cohort study of terminally ill cancer patients. *Journal of pain and symptom management* **31**, 493-501, doi:10.1016/j.jpainsymman.2005.11.014 (2006).
- 28 Mishima, Y., Nagasaki, E., Terui, Y., Irie, T., Takahashi, S., Ito, Y. *et al.* Combination chemotherapy (cyclophosphamide, doxorubicin, and vincristine with continuous-infusion cisplatin and etoposide) and radiotherapy with stem cell support can be beneficial for adolescents and adults with esthesioneuroblastoma. *Cancer* **101**, 1437-1444 (2004).
- 29 Weiser, M. A., Cabanillas, M. E., Konopleva, M., Thomas, D. A., Pierce, S. A., Escalante, C. P. *et al.* Relation between the duration of remission and hyperglycemia during induction chemotherapy for acute lymphocytic leukemia with a hyperfractionated cyclophosphamide, vincristine,

- doxorubicin, and dexamethasone/methotrexate–cytarabine regimen. *Cancer* **100**, 1179-1185 (2004).
- 30 Messinger, Y., Gaynon, P., Raetz, E., Hutchinson, R., DuBois, S., Glade-Bender, J. *et al.* Phase I study of bortezomib combined with chemotherapy in children with relapsed childhood acute lymphoblastic leukemia (ALL): a report from the therapeutic advances in childhood leukemia (TACL) consortium. *Pediatric blood & cancer* **55**, 254-259 (2010).
- 31 Bonate, P. L. Nonlinear mixed effects models: Theory. *Pharmacokinetic-pharmacodynamic modeling and simulation*, 205-265 (2006).
- 32 Ette, E. I., Williams, P. J., Kim, Y. H., Lane, J. R., Liu, M. J. & Capparelli, E. V. Model appropriateness and population pharmacokinetic modeling. *Journal of clinical pharmacology* **43**, 610-623 (2003).
- 33 Almufti, R., Wilbaux, M., Oza, A., Henin, E., Freyer, G., Tod, M. *et al.* A critical review of the analytical approaches for circulating tumor biomarker kinetics during treatment. *Annals of oncology* **25**, 41-56 (2014).
- 34 Malkan, U. Y., Gunes, G., Isik, A., Eliacik, E., Etgul, S., Aslan, T. *et al.* Rebound Thrombocytosis following Induction Chemotherapy Is an Independent Predictor of a Good Prognosis in Acute Myeloid Leukemia Patients Attaining First Complete Remission. *Acta Haematol-Basel* **134**, 32-37, doi:10.1159/000369917 (2015).
- 35 Bowman, W. P., Shuster, J. J., Cook, B., Griffin, T., Behm, F., Pullen, J. *et al.* Improved survival for children with B-cell acute lymphoblastic leukemia and stage IV small noncleaved-cell lymphoma: a pediatric oncology group study. *Journal of clinical oncology : official journal of the American Society of Clinical Oncology* **14**, 1252-1261 (1996).
- 36 Patel, J. N. & Papachristos, A. Personalizing chemotherapy dosing using pharmacological methods. *Cancer Chemoth Pharm* **76**, 879-896, doi:10.1007/s00280-015-2849-x (2015).
- 37 Wählby, U., Jonsson, E. N. & Karlsson, M. O. Comparison of stepwise covariate model building strategies in population pharmacokinetic-pharmacodynamic analysis. *Aaps Pharmsci* **4**, 68-79 (2002).

ABSTRACT (IN KOREAN)

소아청소년 항암치료에서 바이오마커기반 질병진행 예측모형 개발

< 지도교수 박 경 수 >

연세대학교 대학원 의과학과

허영아

목적

본 연구의 목적은 급성 림프구성 백혈병 소아 환자들에게서 바이오마커 기반 질병진행을 예측할 수 있는 모형을 모델링 하고 모델 매개변수 추정치와 환자의 공변량을 이용하여 환자의 생존 기간을 예측하여 향후 환자 개인별 특성을 고려한 급성 림프구성 백혈병 환자의 질병관리 또는 적절한 항암요법을 선택하는데 활용하고자 한다.

방법

본 연구는 후향적 연구로서 2000 년 1 월 1 일 ~ 2015 년 7 월 31 일의 기간 동안 연세의료원 세브란스병원에서 급성 림프모구 백혈병 소아암으로 진단받고 치료받은 환자들의 전자의무기록 (electronic medical record, EMR) 에서 수집된 총 74 명의 자료를 분석하였다. 유효성 평가를 위한 biomarker 은 기존 연구에서 급성 림프모구 백혈병 예후인자로 알려진 혈소판 및 림프구 수치를 사용하였다. 질병이 진행됨에 따라 혈소판은 감소하고 림프구는 증가한다는 가정하에 항암치료 효과는 disease progression model 로 모델링 하였다. 공변량 분석에는 stepwise 방법을 사용하여 환자의 나이, 백혈구 수, creatinine, AST, ALT 등의 유의성을 평가하였으며 forward inclusion 과 backward elimination 의 유의도는 각각 0.05 와 0.01 로 설정하였다³⁷.

자료의 분석 및 모형 구축에는 비선형혼합효과 모델링에 기반을 둔 NONMEM 7.3 version (ICON Development Solutions, MD)이 사용되었으며 필요에 따라 Wings for NONMEM, Perl-Speaks-NONMEM (PSN), R 등의 프로그램이 사용되었다.

개발된 모형의 평가는 Visual predictive check (VPC) 를 통한 시뮬레이션 자료와 실제 자료 사이의 유사성으로부터 모형의 예측능력을 확인하는 것으로 진행하였다.³¹ 아울러 생존 모형은 각 시간에서의 환자의 실제 생존 여부와 모형에서 예측된 생존 확률을 시각적으로 비교하는 것으로 평가하였다.³²

결과

74 명의 환자들은 임상에서 쓰이는 예후인자에 따라 고위험 (HR)과 표준위험 (SR) 그룹으로 나뉘었다. 개발된 질병진행 모형은 K-PD 모형의 속도상수, 항암제 효능 (Emax 모형로 구현), 바이오마커의 성숙도 (transit 모형로 구현) 그리고 질병진행 상수 등의 파라미터로 구성되었다. 항암치료 효과는 K-PD 모형으로 약물 노출량을 얻은 후 이것을 바탕으로 약물 효과를 Emax 모형로 구축하였다. 얻어진 EC_{50} 파라미터의 값은 ALC 와 PLT 모두 저위험군에 비해 고위험군이 더 높았다. 바이오마커의 성숙에 걸리는 시간 (MTT) 은 림프구는 5.34 일, 혈소판은 17.0 일로 알려져 있는 life span 일수와 비슷하였다. 또한 바이오마커의 생리학적 기전을 반영하기 위해 feedback mechanism 을 적용하였는데, 모형에서는 바이오마커의 증식이 질병의 진행에 따라 변할 수 있고 혈중에서 얻어진 바이오마커의 농도는 그에 반비례하다고 추정하였다. Feedback mechanisms 에서 구해진 gamma 값은 ALC 는 0.0973, PLT 는 0.215 로 PLT 의 피드백이 좀 더 급변하는 것으로 결과가 나왔다. 공변량 분석을 진행한 결과, WBC가 ALC 의 baseline 에 관여하는 것으로 발견 되었고 나이 또한 림프구의 성숙도에 관여하는 것으로 모델링 되었다. 또한 AST,

ALT, creatinine 이 PLT 관련 항암치료약물 반감기에 영향을 주는 것으로 발견되었고 추후 나이가 PLT 의 baseline 에 영향을 주는 것으로 발견되었다. 그 후 질병진행 속도의 30 일 시점에서의 모델 예측치, BMT 과거력, 그리고 ALC 의 22 일 시점까지의 모델 예측치와 baseline 간의 비의 평균값을 공변량으로 대입하여 생존률 예측모형을 개발하였다.

결론

본 결과는 바이오마커를 통하여 급성 림프모구 백혈병의 질병 진행 정도를 예측하고자 하였다. 개발된 바이오마커 질병 진행 예측 모델은 예측치가 관측치와 대체로 일치하였다. 또한 질병 진행 예측 모델을 통해 얻은 파라미터들을 사용하여 개발된 생존모형은 관측된 생존률을 잘 예측하였다. 본 연구는 바이오마커 기반의 질병 진행 예측 모델이 급성 림프모구 백혈병 환자의 질병관리에 활용할 수 있음을 보여준다.

핵심되는말: 급성 림프모구 백혈병 소아암, 바이오마커, 질병진행 모델, 혈소판, 림프구, 생존률 예측모형